JOTCS A
Journal of the Turkish Chemical Society
Section: A
Chemistry
TURKISH CHEMICAL SOCIETY

Optoelectronic Parameters of 2-oxo-2-(1-oxo-1*H*-isochromen-3-yl)ethyl methacrylate Compound Thin Film

Adnan Kurt[1,*], Murat Koca[2]

[1]Department of Chemistry, Faculty of Science and Arts, Adiyaman University, Adiyaman, Turkey
[2]Department of Pharmaceutical Chemistry, Faculty of Pharmacy, Adiyaman University, Adiyaman, Turkey

Abstract: The UV/VIS spectrophotometric scans were obtained to determine the opto-electronic properties of 2-oxo-2-(1-oxo-1*H*-isochromen-3-yl)ethyl methacrylate (other name: 2-(isocoumarin-3-yl)-2-oxoethyl methacrylate) compound thin film. The refractive index of compound at 700 nm was found to be 1.61. The values of the real part of the dielectric constant were higher than those of the imaginary part. The results indicated that the electronic transition responsible for the absorption was the indirect allowed one. The optical band gap constant and the Urbach energy corresponding to the width of the band tails of localized states were calculated to be 3.19 eV and 1.05 eV, respectively. From the results obtained, it is predicted that 2-oxo-2-(1-oxo-1*H*-isochromen-3-yl)ethyl methacrylate (OICEMA) compound can take place in the semiconductor class and play a role in the design of some electro-optic materials.

Keywords: 1*H*-isochromen-1-one, isocoumarin, UV absorptions, optical properties, dispersion parameters

Submitted: November 25, 2021. **Accepted:** April 07, 2022.

Cite this: Kurt A, Koca M. Optoelectronic Parameters of 2-oxo-2-(1-oxo-1H-isochromen-3-yl)ethyl methacrylate Compound Thin Film. JOTCSA. 2022;9(2):613–20.

DOI: https://doi.org/10.18596/jotcsa.1028320.

***Corresponding author. E-mail:** akurt@adiyaman.edu.tr. Tel: 90416 2233800

INTRODUCTION

Isocoumarins or 1*H*-isochromen-1-ones, are the most important members of the heterocyclic compound class, especially in the natural lactam ring compound group (1). The chemical structure of this compound consists of a lactonic α-pyranone ring fused to the benzene ring at positions 5,6 (2). These compounds form the basis of various biologically and pharmacologically important natural products (3). While isocoumarins and derivatives can be used directly by naturally extracting them from many sources, the synthesis of these compounds has also been carried out by using many different synthetic methods . Some of these commonly used methods are conventional synthetic reactions, microwave-assisted reactions, insertion, cyclization, and bond cleavage reactions, and also transition metal catalyzed reactions (3-6). As a result of the use of isocoumarin derivatives as reagents under different reaction conditions, new types of hetero or carboxylic compounds such as isocarbostyrils, isoquinolines, and isochromenes have also been synthesized (3,7). Due to their heterocyclic structures, isocoumarins exhibit important biological-pharmacological and chemical properties (2,8).

Due to the π-conjugated bond system in their structures, isocoumarins and derivatives show electrical-optical properties, and thus they may be candidate compounds for optically active materials similar to their coumarin isomers. So, as it is known, studies on the optical properties and application areas of coumarins, which have π-conjugated bonds, are frequently seen in the literature, and some of them show important optoelectronic properties and can be classified as semiconductor materials (9,10). However, the majority of reported studies on isocoumarins are concentrated on their biological or pharmacological effects. But, there are still some publications investigating the photophysical properties of isocoumarins in literature. For example, Elmas and

coworkers designed a novel fluorescent probe based on an isocoumarin compound, 2-amino-4-phenyl-6-(isocoumarin-3-yl) -3-cyanopyridine, for mercury and iron ions and for live cell imaging applications (11). Pirovano and friends reported the synthesis, characterization and photophysical properties of some isocoumarin derivatives-based D-π-A systems (12). In another study, Shoji and coworkers synthesized various benzofurans and isocoumarins with azulene group using intramolecular cyclization reaction of 1-ethynylazulenes. They clarified the structures of molecules by single-crystal XRD analysis and investigated the optical parameters using UV spectroscopy (13). Zamani and friends also synthesized and characterized some novel optically active 3-substituted isocoumarins and 3,4-dihydroisocoumarins containing L-valine and L-leucine moieties (14).

As mentioned above, mostly the biological activities of isocoumarin molecules have been investigated. In addition to these, the synthesis of polymers based isocoumarin molecules has also been encountered in limited numbers in the literature (1,5,15). In this context, some isocoumarin derived polymer/copolymer systems and their various properties have been reported by our research group in previous studies (5,15). Apart from these aforementioned properties of isocoumarins, studies investigating the optical properties of isocoumarin derivatives in detail have not been found within our knowledge of the literature. In order to make a contribution to the existing literature deficiency on the electro-optical properties of isocoumarins or 1H-isochromen-1-ones, herein we aim that UV measurements of 2-oxo-2-(1-oxo-1*H*-isochromen-3-yl)ethyl methacrylate (OICEMA) compound are recorded in the wavelength range of 330 - 700 nm. Some optical parameters are calculated using the related equations available in the literature. From the results obtained, it is predicted that OICEMA compound can take place in the semiconductor class and play a role in the design of some electro-optical materials.

EXPERIMENTAL

Materials

The used solvents, dimethyl sulfoxide (DMSO), tetrahydrofuran (THF), chloroform, and ethanol were purchased from Sigma-Aldrich. In addition, the synthesis of OICEMA compound was achieved again by the reaction of 3-(bromoacetyl)-1*H*-isochromen-1-one and sodium methacrylate in the presence of THF as well as following a series of experimental steps according to our previous studies (5,15). Schematic representation of OICEMA compound was illustrated in Figure 1. The FTIR and ^{1}H-NMR data are summarized below:

FTIR (cm^{-1}): 1601 (aromatic C=C), 1634 (vinyl C=C), 1708 (acetyl ketone C=O), 1722 (isocoumarin ring C=O), 1741 (methacrylate C=O), 2993–2853 (aliphatic C-H), 3111–3041 (aromatic C-H).

^{1}H-NMR (DMSO, δppm): 1.95 (vinyl -CH_3), 5.45 (–$COOCH_2$), 5.82 and 6.17 (vinyl =CH_2), 7.78 - 8.01 (aromatic =CH-), 8.27 (isocoumarin =CH-).

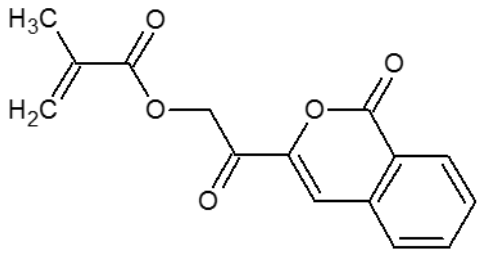

Figure 1: Scheme of OICEMA compound.

Instrumental Techniques

Spectral characterizations were performed with a Perkin Elmer Spectrum 100 FTIR (ATR) spectrometer and a Bruker 300 Mhz Ultrashield TM nuclear magnetic resonance spectrometer. A thin film of compound was prepared with spin coating technique. Therefore, a Laurell WS-400-6NPP-Lite spin coater was used. For this process, 0.025 gram of OICEMA compound was weighed and dissolved in 25 mL of dimethyl sulfoxide and coated onto a glass at the conditions of 5 bar argon gas pressure and 2500 rpm for 25 seconds. The thickness of film was measured to be 2 μm using a digital micrometer supplied by Mitutoyo Corporation Ltd Japan. Then, UV measurements were carried out by a Perkin Elmer Lambda 25 UV/VIS Specrophotometer (330 – 700 nm).

RESULTS AND DISCUSSION

The spectral characterization of the OICEMA compound was re-achieved with FTIR and ^{1}H-NMR techniques according to our previous studies (5,15). Figure 2 shows the FTIR spectrum of the compound in which the most characteristic bands are observed at 3111–3041 cm^{-1} (aromatic C-H), 2993–2853 cm^{-1} (aliphatic C-H), 1741 cm^{-1} (methacrylate C=O), 1722 cm^{-1} (isocoumarin ring C=O), 1708 cm^{-1} (acetyl ketone C=O), 1634 cm^{-1} (vinyl C=C), 1601 cm^{-1} (aromatic C=C).

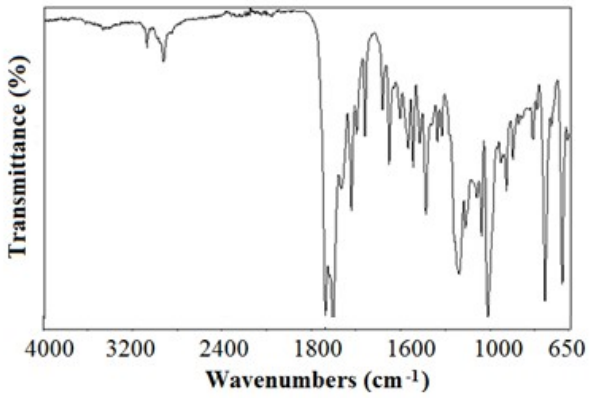

Figure 2: FTIR spectrum of OICEMA compound.

In its ^{1}H-NMR spectrum (Figure 3), the signal at 8.27 ppm is attributed to the =CH- proton in the isocoumarin ring. The chemical shifts between 8.01 ppm and 7.78 ppm are due to the aromatic =CH- protons. Both signals at 6.17 and 5.82 ppm are attributed to vinylic $=CH_2$ protons. The signal at 5.45 ppm is reasoned by CH_2 protons adjacent to the methacrylate ester and the signal at 1.95 ppm is also due to the $-CH_3$ protons adjacent to the vinyl group.

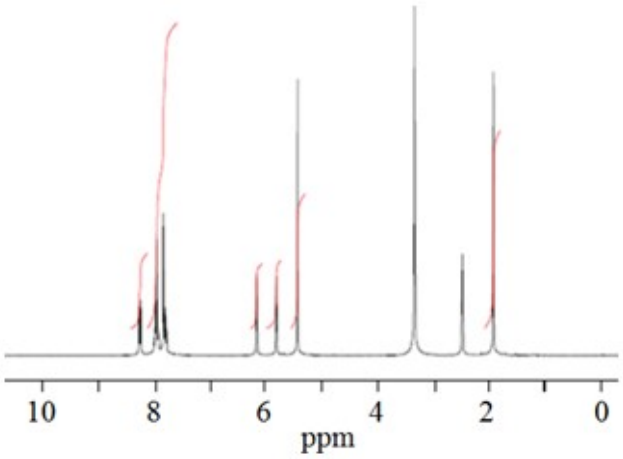

Figure 3: ^{1}H-NMR spectrum of OICEMA compound.

The optical properties of organic molecules containing multiple π–bonds are reported due to their opto-electronic applications (9,10). In order to determine the optical and electronic properties of molecules, UV–VIS spectroscopy is commonly used (16). Some physical phenomena occur when light passes from an air medium to any dense medium, such as a solid phase. That is, the fractions of incident light are partially reflected, transmitted, or absorbed (16). This situation can be formulated as: (T + R + A = 1) where T: transmittance, R: reflectance, and A: absorbance. Using these values, a different set of optical parameters can be easily obtained.

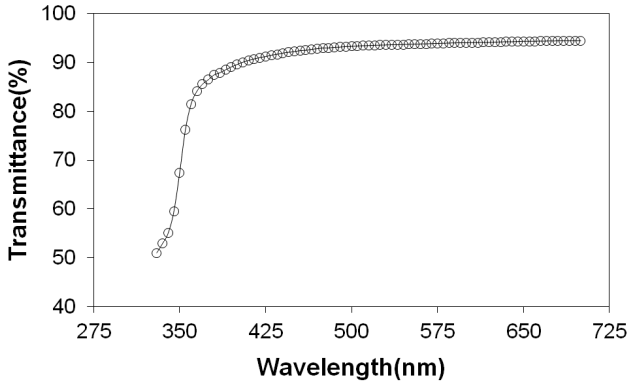

Figure 4: Transmittance spectrum of OICEMA compound.

Therefore, the UV/VIS measurements were obtained between 330 nm and 700 nm for OICEMA compound film. Its transmittance and reflectance spectra were shown in Figures 4 and 5, respectively. Transmittance spectrum was increased depending on the increase in wavelength whereas the reflectance values were decreased. In addition, the results obtained from the UV absorption data showed that the absorption rate in the visible region was less than that of the UV region (17). The absorption exhibited by the OICEMA compound around 330 nm may be reasoned from n-π* transitions of C=O groups in the molecule (18).

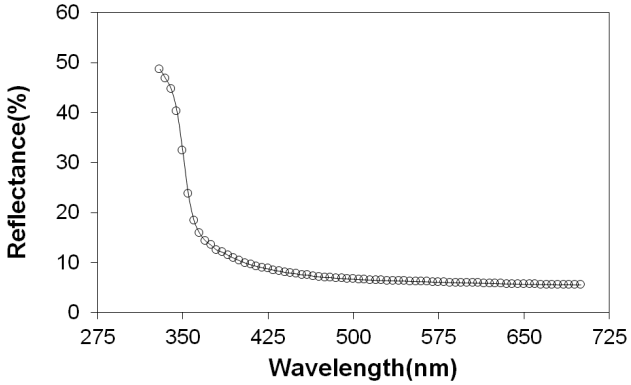

Figure 5: Reflectance spectrum of OICEMA compound.

The refractive index (n) is an important optical parameter and it may be easily determined from the transmittance and reflectance. Therefore, a relationship between these parameters can be explained by the following formula (19):

$$n=\left[\frac{1+R}{1-R}\right]+\left[\frac{4R}{(1-R)^2}-k^2\right]^{1/2} \qquad (1)$$

Where k is the extinction coefficient. This parameter is also obtained as:

$$k=\frac{\alpha\lambda}{4\pi} \quad (2)$$

Where α is the absorption coefficient and corresponds to the following equation:

$$\alpha=\frac{2.303A}{d} \quad (3)$$

Where d is the film thickness, and A is the absorbance. Figure 6 shows that the refractive index is inversely related to the wavelength. Depending on the increase in wavelength, a significant decrease in the refractive index was observed. In particular, this decrease is sharper and more pronounced in the UV region, as pointed out by Rodriguez et al (20). Towards the next wavelengths (after about 400 nm) the decreasing rate is slower and reaches an almost constant value. The n value is found to be 1.61 at 700 nm.

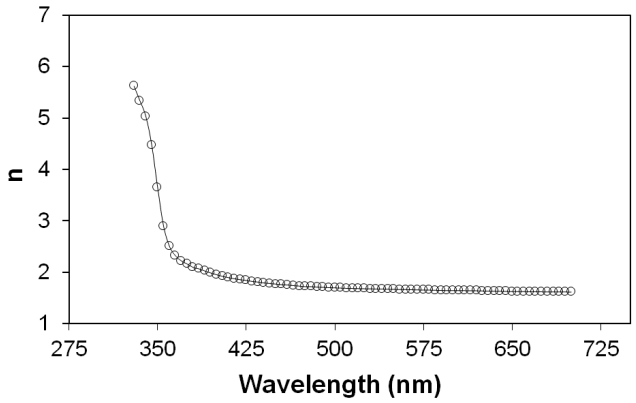

Figure 6: Refractive index dispersion curve of OICEMA compound.

Figure 7 shows the variation of the extinction coefficient with the wavelength. As seen in Figure 7, at the low wavelength range, the decrease in the extinction coefficient is quite evident. However, a stabilization towards higher wavelengths is observed.

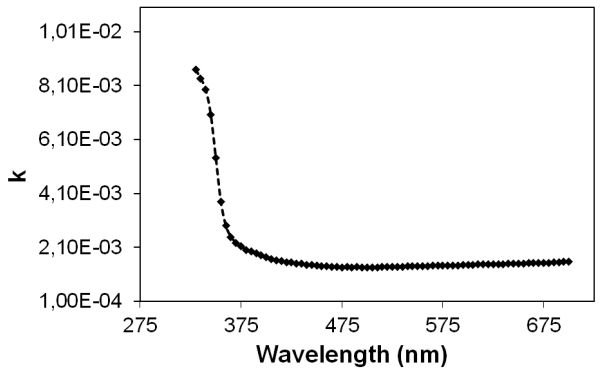

Figure 7: Variation of extinction coefficient (k) as a function of wavelength of OICEMA compound.

The real (ε_r) and imaginary (ε_i) parts of the dielectric constant are:

$$\epsilon_r=n^2-k^2 \quad \text{and} \quad \epsilon_i=2nk \quad (4)$$

The variation of these constants with energy is given in Figure 8. As can be seen from this figure, the imaginary part of dielectric constant is smaller than the real part. The real and imaginary parts values of OICEMA compound were found to be 2.68 and 0.0048 at an energy level of 2 eV, respectively.

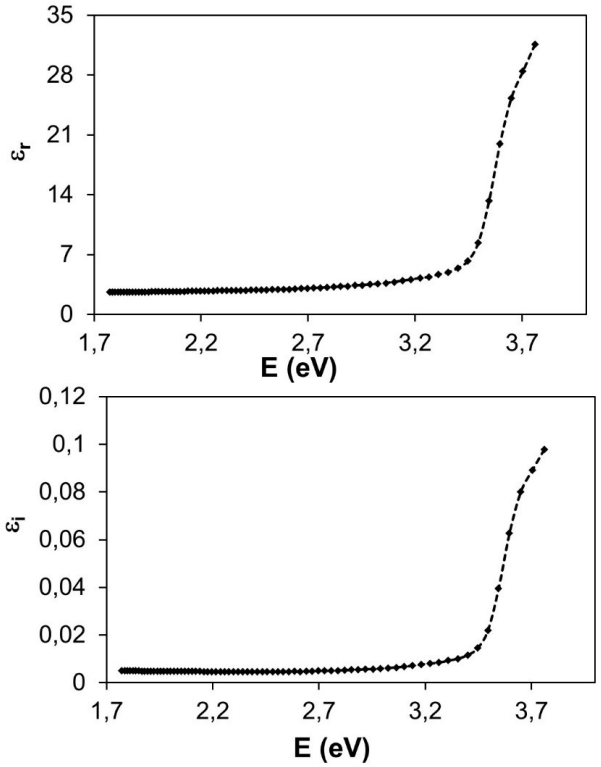

Figure 8: The spectra of real (ε_r) and imaginary (ε_i) parts of dielectric constant of OICEMA compound.

Dispersion energy parameters are obtained by the Wemple and DrDomenico relationship (21). The relationship between *n* and single oscillator strength is evaluated according to following relation:

$$n^2(h\nu)=1+\frac{E_0E_d}{E_0^2-(h\nu)^2} \quad (5)$$

Where E_o is the single – oscillator energy, E_d is the dispersion energy. E_o is responsible of the electronic excitations in the compounds and shows the average of the optical band gap. E_d indicates the dispersion energy in the compounds and shows the average strength of interband optical transition (22). Figure 9 shows the plots $(n^2-1)^{-1}$ versus $(h\nu)^2$ values. The linear fit of this figure yields a slope equal to $(E_oE_d)^{-1}$ and an intercept equal to E_o/E_d. The values of E_o and E_d for OICEMA compound were

found to be 3.96 eV and 4.33 eV, respectively. These values were also listed in Table 1.

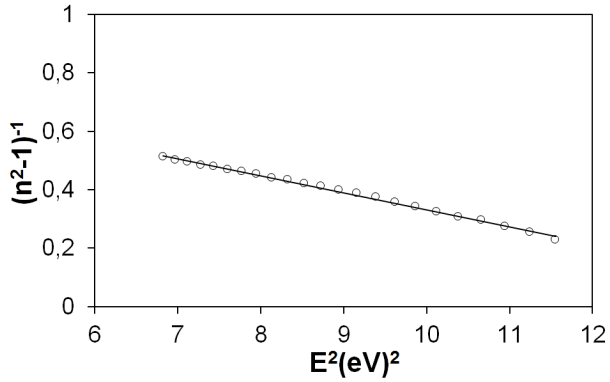

Figure 9: Variation of $(n^2-1)^{-1}$ as a function of E^2 of OICEMA compound.

M_{-1} and M_{-3} moments of the imaginary part of the optical band (21,23) may be defined as: $E_o^2 = M_{-1}/M_{-3}$ and $E_d^2 = (M_{-1})^3/M_{-3}$. Table 1 includes these values. It is noted that M_{-1} value is greater than the M_{-3} when compared to each other.

The single-term Sellmeier relation is used in order to determine the relationship between the refractive index and the wavelength (24):

$$n^2(\lambda)-1=\frac{S_0\lambda_0^2}{1-(\lambda_0/\lambda)^2} \qquad (6)$$

Where λ_o and S_o are the average interband oscillator wavelength and oscillator strength, respectively. To determine both parameters, $(n^2-1)^{-1}$ values against λ^{-2} values according to Eq. (6) are plotted. These plots are shown in Figure 10. From the slope and intercept of line, the S_o and λ_o values of OICEMA compound are calculated and given in Table 1.

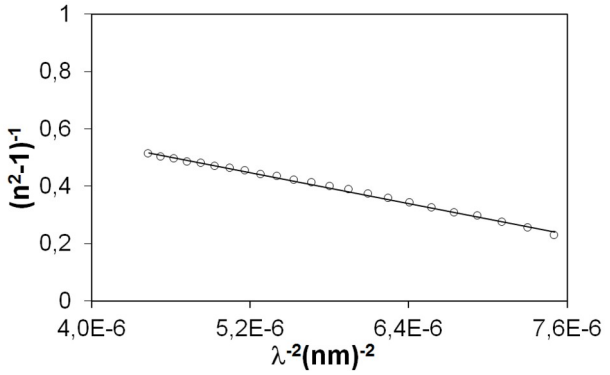

Figure 10: Variation of $(n^2-1)^{-1}$ as a function of $(\lambda)^{-2}$ of OICEMA compound.

In order to understand the interband transition theory of solid state materials, the absorption data at the fundamental edge can be easily analyzed with the following equation (25):

$$(\alpha h\nu)=B(h\nu-E_0)^n \qquad (7)$$

Where E_g is the optical band gap, B is a constant, and n is an index that shows the types of electronic transitions. These n values can take different values, like 2, 3, 1/2, and 3/2. Their interpretations are well known in the literature (22). In order to determine the electronic transition type of any material, the value with the best agreement between the n values should be determined. For this, the $(\alpha h\nu)^{1/n}$ values against energy (hv) values for each n value are plotted and the n value with the best linear regression value is selected. In our work, we achieved the best fit for n=2, that is, for indirect allowed transition for OICEMA compound. Accordingly, $(\alpha h\nu)^{1/2}$ versus (hv) values were plotted in order to calculate the optical band gap (Eg). This is shown in Figure 11. From the extrapolation of this line, the Eg value was calculated as 3.19 eV.

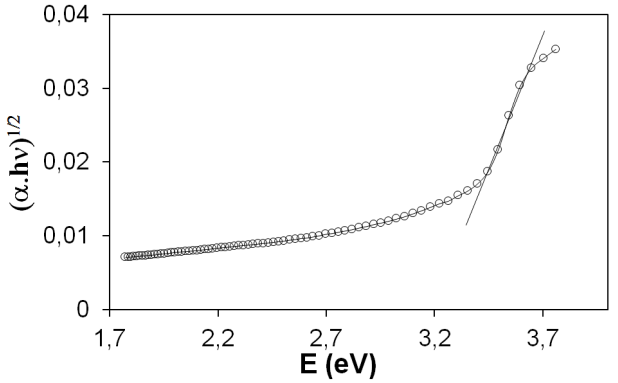

Figure 11: Plot of $(\alpha h\nu)^{1/2}$ vs. E of OICEMA compound.

Table 1: Optical parameters of OICEMA compound.

Eu (eV)	**Eg (eV)**	**E_0 (eV)**	**E_d (eV)**	**$S_0.10^{13}(m^{-2})$**	**λ_0(nm)**
1.05	3.19	3.96	4.33	1.11	313
M_{-1}	**$M_{-3}(eV)^{-2}$**	**β**	**α_0**	**n (700 nm)**	**T% (700 nm)**
1.09	0.07	0.025	$2.88.10^{-6}$	1.61	94.48

When any material is exposed to a certain UV wavelength, some localized defect states can occur in the band gap. These defect states can trap the excited electrons and prevent their direct transition to the conduction band (26). The tail width of these defect states is defined as the Urbach energy and can be determined by the following general formula (27):

$$\alpha = \alpha_0 \exp\left(\frac{E}{E_u}\right) \quad (8)$$

Where α_0 is a constant, and E_u is the Urbach energy. The slope of the line obtained from the graph of (ln α) versus energy E (eV) can be used to calculate it. This is shown in Figure 12. The value of Urbach energy was calculated to be 1.05 eV while α_0 constant was $2.88x10^{-6}$. In addition, at a constant temperature and in the Urbach tail range, the slope of Figure 10 corresponds to σ/kT. Where k is the Boltzmann constant, and T is the temperature, σ is the steepness parameter. This parameter is temperature dependent and characterizes the broadening of absorption edge. This state is usually caused by electron-phonon interactions (28). The steepness parameter of OICEMA compound is calculated as 0.0245 when T is 298 K.

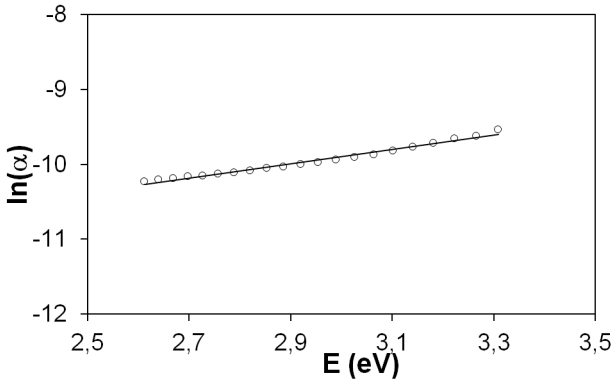

Figure 12: Plot of lnα vs. E of OICEMA compound.

CONCLUSIONS

The UV measurements of 2-oxo-2-(1-oxo-1*H*-isochromen-3-yl)ethyl methacrylate compound were recorded to determine some optical and dispersion parameters. Transmittance was increased depending on the increase in wavelength, whereas the reflectance values were decreased. The refractive index and wavelength were inversely related, and a significant decrease was observed in the refractive index with increasing wavelength. The refractive index at 700 nm was 1.61. The real and imaginary part values were found to be 2.68 and 0.0048 at the energy level of 2 eV, respectively. For compounds, the type of electronic transition allowed was the indirect one. The optical band gap constant and the Urbach energy were calculated to be 3.19 eV and 1.05 eV, respectively. These results show that 2-oxo-2-(1-oxo-1*H*-isochromen-3-yl)ethyl methacrylate can take place in the semiconductor class and play a role in the design of some electro-optical materials.

REFERENCES

1. Han T, Deng H, Yu CYY, Gui C, Song Z, Kwok RTK, et al. Functional isocoumarin-containing polymers synthesized by rhodium-catalyzed oxidative polycoupling of aryl diacid and internal diyne. Polym Chem. 2016;7(14):2501–10. <DOI>.

2. Saeed A. Isocoumarins, miraculous natural products blessed with diverse pharmacological activities. European Journal of Medicinal Chemistry. 2016 Jun;116:290–317. <DOI>.

3. Saikia P, Gogoi S. Isocoumarins: General Aspects and Recent Advances in their Synthesis. Adv Synth Catal. 2018 Jun 5;360(11):2063–75. <DOI>.

4. Pal S, Chatare V, Pal M. Isocoumarin and Its Derivatives: An Overview on their Synthesis and Applications. COC. 2011 Mar 1;15(5):782–800. <DOI>.

5. Kurt A, Kılınç İ, Koca M. Preparation of Copolymer Systems of 2-(Isocoumarin-3-yl)-2-oxoethyl Methacrylate with Methyl Methacrylate and Thermal Decomposition Kinetics. Iran J Sci Technol Trans Sci. 2020 Aug;44(4):1039–50. <DOI>.

6. Koca M, Ertürk AS, Umaz A. Microwave-assisted intermolecular aldol condensation: Efficient one-step synthesis of 3-acetyl isocoumarin and optimization of different reaction conditions. Arabian Journal of Chemistry. 2018 May;11(4):538–45. <DOI>.

7. Barry RD. Isocoumarins. Developments since 1950. Chemical Reviews. 1964;64(3):229–60.

8. Tian JF, Li PJ, Li XX, Sun PH, Gao H, Liu XZ, et al. New antibacterial isocoumarin glycosides from a wetland soil derived fungal strain Metarhizium anisopliae. Bioorganic & Medicinal Chemistry Letters. 2016 Mar;26(5):1391–6. <DOI>.

9. Bai Y, Du J, Weng X. Synthesis, characterization, optical properties and theoretical calculations of 6-fluoro coumarin. Spectrochimica Acta Part A: Molecular and Biomolecular Spectroscopy. 2014 May;126:14–20. <DOI>.

10. Kurt A, Gündüz B, Koca M. A detailed study on the optical properties of 3-benzoyl-7-hydroxy coumarin compound in different solvents and concentrations. Maced J Chem Chem Eng. 2019 Dec 30;38(2):227. <DOI>.

11. Karuk Elmas SN, Dincer ZE, Erturk AS, Bostanci A, Karagoz A, Koca M, et al. A novel fluorescent probe based on isocoumarin for Hg2+ and Fe3+ ions and its application in live-cell imaging. Spectrochimica Acta Part A: Molecular and Biomolecular Spectroscopy. 2020 Jan;224:117402. <DOI> .

12. Pirovano V, Marchetti M, Carbonaro J, Brambilla E, Rossi E, Ronda L, et al. Synthesis and photophysical properties of isocoumarin-based D-π-A systems. Dyes and Pigments. 2020 Feb;173:107917. <DOI>.

13. Shoji T, Tanaka M, Takagaki S, Miura K, Ohta A, Sekiguchi R, et al. Synthesis of azulene-substituted benzofurans and isocoumarins *via* intramolecular cyclization of 1-ethynylazulenes, and their structural and optical properties. Org Biomol Chem. 2018;16(3):480–9. <DOI>.

14. Zamani K, Faghihi K, Ebrahimi S. Synthesis of Some Novel Optically Active Isocoumarin and 3,4-Dihydroisocoumarin Containing L-valine and L-leucine Moieties. Turk J Chem. 2005;29:171–5. <URL>.

15. Kurt A, Avci HI, Koca M. Synthesis and characterization of a novel isocoumarin derived polymer and its thermal decomposition kinetics. Maced J Chem Chem Eng [Internet]. 2018 Dec 3 [cited 2022 Apr 16];37(2). <DOI>.

16. Aziz SB, Brza MA, Nofal MM, Abdulwahid RT, Hussen SA, Hussein AM, et al. A Comprehensive Review on Optical Properties of Polymer Electrolytes and Composites. Materials. 2020 Aug 20;13(17):3675. <DOI>.

17. Rawat A, Mahawar H, Chauhan S, Tanwar A, Singh P. Optical band gap of polyvinylpyrrolidone/polyacrilamide blend thin films. IJPAP. 2012;50:100–4. <URL>.

18. Zidan HM, Abu-Elnader M. Structural and optical properties of pure PMMA and metal chloride-doped PMMA films. Physica B: Condensed Matter. 2005 Jan;355(1–4):308–17. <DOI>.

19. Atyia H. Influence of deposition temperature on the structural and optical properties of InSbSe~ 3 films. Journal of optoelectronics and advanced materials. 2006;8(4):1359.

20. Rodŕiguez J, Gómez M, Ederth J, Niklasson GA, Granqvist CG. Thickness dependence of the optical properties of sputter deposited Ti oxide films. Thin Solid Films. 2000 Apr;365(1):119–25. <DOI>.

21. Wemple SH, DiDomenico M. Behavior of the Electronic Dielectric Constant in Covalent and Ionic Materials. Phys Rev B. 1971 Feb 15;3(4):1338–51. <DOI>.

22. Veena G, Lobo B. Dispersive parameters of oxidized PVA-PVP blend films. Turkish Journal of Physics. 2019 Aug 1;43(4):337–54. <URL>.

23. Ammar AH. Studies on some structural and optical properties of ZnxCd1−xTe thin films. Applied Surface Science. 2002 Nov;201(1–4):9–19. <DOI>.

24. DrDomenico M, Wemple SH. Oxygen-Octahedra Ferroelectrics. I. Theory of Electro-optical and Nonlinear optical Effects. Journal of Applied Physics. 1969 Feb;40(2):720–34. <DOI>.

25. Tauc J, editor. Amorphous and Liquid Semiconductors. New York: Plenum Press; 1974.

26. Akshay VR, Arun B, Mandal G, Vasundhara M. Visible range optical absorption, Urbach energy estimation and paramagnetic response in Cr-doped TiO_2 nanocrystals derived by a sol–gel method. Phys Chem Chem Phys. 2019;21(24):12991–3004. <DOI>.

27. Urbach F. The Long-Wavelength Edge of Photographic Sensitivity and of the Electronic Absorption of Solids. Phys Rev. 1953 Dec 1;92(5):1324–1324. <DOI>.

28. Abu El-Fadl A, Soltan AS, Shaalan NM. Temperature dependence of the indirect band gap, steepness parameter and related optical constants of [Kx(NH4)1−x]2ZnCl4 mixed crystals. Optics & Laser Technology. 2007 Oct;39(7):1310–8. <DOI>.